Tracing Diagnosis Paths on Histopathology WSIs for Diagnostically Relevant Case Recommendation

Yushan Zheng[1], Zhiguo Jiang[2,1], Haopeng Zhang[2,1], Fengying Xie[2,1], and Jun Shi[3]

[1] Beijing Advanced Innovation Center for Biomedical Engineering, Beihang University, Beijing 100191, China. yszheng@buaa.edu.com
[2] Image Processing Center, SA, Beihang University, Beijing, 102206, China.
[3] School of Software, Hefei University of Technology, Hefei 230601, China.

Abstract. Telepathology has enabled the remote cancer diagnosis based on digital pathological whole slide images (WSIs). During the diagnosis, the behavior information of the pathologist can be recorded by the platform and then archived with the digital cases. The diagnosis path of the pathologist on a WSI is valuable information since the image content within the path is highly correlated with the diagnosis report of the pathologist. In this paper, we proposed a novel diagnosis path network (DPathNet). DPathNet utilizes the diagnosis paths of pathologists on the WSIs as the supervision to learn the pathology knowledge from the image content. Based on the DPathNet, we develop a novel approach for computer-aided cancer diagnosis named session-based histopathology image recommendation (SHIR). SHIR summaries the information of a WSI while the pathologist browsing the WSI and actively recommends the relevant cases within similar image content from the database. The proposed approaches are evaluated on a gastric dataset containing 983 cases within 5 categories of gastric lesions. The experimental results have demonstrated the effectiveness of the DPathNet to the SHIR task and the supervision of the diagnosis path is sufficient to train the DPathNet. The MRR and MAP of the proposed SHIR framework are respectively 0.741 and 0.777 on the gastric dataset.

Keywords: Digital pathology · Gastric cancer · Recommendation.

1 Introduction

With the development of whole slide imaging and digital pathology, the biopsy sections have been well archived and the artificial intelligent methods for histopathological whole slide image analysis are widely developed [1,4]. There are two remarkable research interests in recent studies on histopathological image analysis (HIA). The one is to develop weak-supervision [2] frameworks to relieve the annotation load of the pathologists [7]. Another is to utilize the resource of digital pathology platforms to enrich the information [9] of auxiliary diagnosis. With the increasing application of the telepathology system, abundant

diagnosed cases have been accumulated. The cases contain not only the WSIs but also valuable data including the diagnosis report, meta information, user behavior data, etc. These data are potential to develop CAD applications that are both light-annotated and informative.

One notable information in the telepathology platform is the browse path on the WSI during the diagnosis, which can be automatically recorded by the digital platform without disturbing the pathologists. Theoretically, the pathologist should have reviewed the conclusive regions related to a specific disease before making the diagnosis. Therefore, the diagnosis path on the WSI and the diagnosis result should be highly correlated. This hypothesis motivated us to build a deep neural network to learn the relationship between image content under the diagnosis path and the label of the WSI, and verify whether this type of weak supervision is sufficient to learn pathology knowledge and build computer-aided cancer diagnosis system.

In this paper, we propose a novel deep learning framework to learn pathology knowledge based on the path of diagnosis on WSIs. Furthermore, we proposed a novel approach for computer-aided diagnosis named session-based histopathology image recommendation (SHIR). As shown in Figure 1, the application is designed to monitor the pathologist's browse path on the WSI during diagnosis and actively query the telepathology database to recommend historical cases within relevant path and image content. The similar cases are fed to the pathologist to provide assistant information. We have conducted experiments to verify the proposed method and compared it with related methods [15,20,18] on a large scale gastric dataset. The experimental results have demonstrated the supervision of the diagnosis path is sufficient to train a qualified model for histopathological image analysis, and the proposed SHIR is promising to develop systems for computer-aided cancer diagnosis.

The contribution of this paper is two-fold. 1) We proposed a novel DPathNet, which utilized the browse paths on the WSIs as the supervision to learn the pathology knowledge from WSIs. The training of DPathNet does not rely on the pixel-level or image-level annotations. The annotation workload is much lighter than that in traditional methods. 2) We introduced the technique of session-based recommendation [10,17] into the domain of histopathological image analysis and developed the session-based histopathology image recommendation (SHIR). The data for training and application of the SHIR can be automatically formed by the telepathology platform without disturbing the diagnosis of pathologists.

2 Related works

Recommendation is an important task in online services (e.g. e-commerce, media streaming), which traces the browsing history of a customer and feeds back the relevant items to the customer for reference. In the domain of histopathological image analysis, the most related existing application is content-based histopathological image retrieval (CBHIR) [9,12,11,22]. CBHIR can provide more

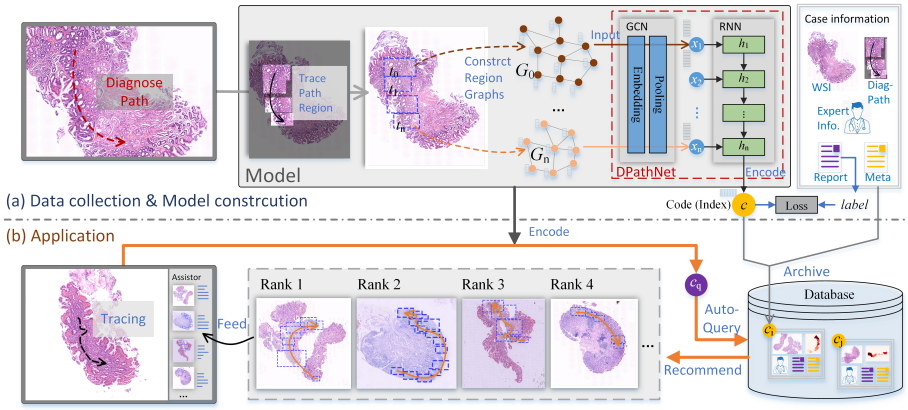

Fig. 1. The framework of the proposed recommendation approach. (a) presents the flowchart of the model construction, where the ROIs in the diagnosis path are numbered and the features of ROIs are extracted using GCNs, then the sequence of features are fed into an RNN to obtain the code of the path. (b) illustrates an application instance, where the diagnosis path is encoded using the trained model and then the relevant cases are recommended based on similarity measurement.

interpretable information than the traditional applications, e.g. segmentation, detection, to the pathologists [21,13,5,6]. However, CBHIR requires the pathologists manually selecting a region of interest (ROI) as the query instance and the retrieval does not consider the regions the pathologists have already viewed. In comparison, the proposed recommendation framework can continuously analyze the intention of the pathologists throughout the diagnosis and actively feed back the relevant cases to pathologists. The application is more informative and convenient than the CBHIR.

In the aspect of machine learning techniques, graph convolution networks (GCNs) and recurrent neural networks (RNNs) are introduced into the domain of histopathology image analysis in recent years and have proven effective in the tasks of large histopathology image encoding and recognition. Li et al. [8] utilized graphs for survival analysis based on WSI. Zheng et al. [20] applied a GCN to encode the sub-regions on the WSI for CBHIR. Campanella et al. [2] employed RNNs to combine the information of key patches in the feature space and Yan et al. [18] used RNNs to model the adjacency of patches for histopathological image classification. In our method, GCN is utilized to encode the ROIs in the diagnosis path and RNN is employed to mine the pathology information based on the features of the sequential ROIs.

3 Method

The proposed SHIR framework is illustrated in Figure 1, where the DPathNet is the main component in the framework. The feature extraction for ROIs within

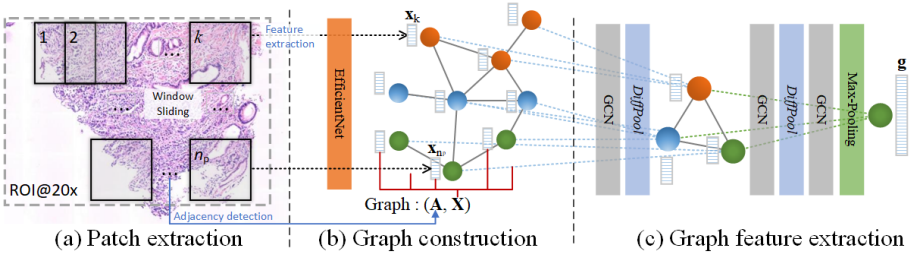

Fig. 2. The flowchart of region feature extraction, where (a) displays an ROI in a diagnosis path and the window sliding strategy on the region, (b) illustrates the items for graph construction, and (c) is structure of the GCN for graph feature extraction.

the path and the encoding of the sequential browsing information are the main tasks of DPathNet, which will be detailed in this section.

3.1 ROI feature extraction

The features to represent image regions within the diagnosis path are extracted based on GCNs following Zheng et al.[20]. As shown in Figure 2, an ROI is divided into patches using a sliding window and the patches are fed into a CNN to extract patch features. The CNN structure is the EfficientNet [14] for its good performance in image classification tasks. The resolution to extract the features is 0.48μm/pixel (under $20\times$ lens). Letting $\mathbf{x}_k \in \mathbb{R}^d$ denote the CNN feature of the k-th patch, the graph for the ROI is defined as $G = (\mathbf{A}, \mathbf{X})$, where $\mathbf{A} \in \{0,1\}^{n_p \times n_p}$ is the 4-neighborhood adjacency matrix for the n_p patches in the ROI and $\mathbf{X} = [\mathbf{x}_1, ..., \mathbf{x}_{n_p}] \in \mathbb{R}^{d \times n_p}$ is the feature matrix of the graph[4]. Next, the graph is fed into a hierarchical GCN structures with DiffPool modules[19] to extract the graph feature. The process is represented in brief as $\mathbf{g} = \mathcal{F}_{graph}(\mathbf{A}, \mathbf{X})$ in this paper and the details for the graph feature extraction please refer to the *Supplemental Material*.

3.2 Diagnosis path encoding

The encoding of the path is based on an RNN. In this paper, we selected the Gated Recurrent Units (GRU)[3] to build the RNN. Here, the features of the sequential ROIs are represented as $S = \{\mathbf{g}_1, \mathbf{g}_2, ..., \mathbf{g}_n\}$. Letting S be the input of the RNN, the inference of the GRU at time $t = 1, 2, .., n$ is defined as

$$\begin{aligned} &\mathbf{z}_t = \sigma(\mathbf{W}_z \mathbf{g}_t + \mathbf{U}_z \mathbf{h}_{t-1}), \mathbf{r}_t = \sigma(\mathbf{W}_r \mathbf{g}_t + \mathbf{U}_r \mathbf{h}_{t-1}), \\ &\tilde{\mathbf{h}} = \tanh(\mathbf{W}\mathbf{g}_t + \mathbf{U}(\mathbf{r}_t \odot \mathbf{h}_{t-1})), \mathbf{h}_t = (1 - \mathbf{z}_t) \odot \mathbf{h}_{t-1} + \mathbf{z}_t \odot \tilde{\mathbf{h}}, \end{aligned} \tag{1}$$

where $\mathbf{z}_t$ and $\mathbf{r}_t$ are respectively the update gate and the reset gate, the notations involving $\mathbf{W}$ and $\mathbf{U}$ are trainable parameters, $\odot$ represents the Hadamard product, and $\mathbf{h}_t$ is the activation at time t ($\mathbf{h}_0 = \mathbf{0}$). Correspondingly, $\mathbf{h}_n$ is the final output of the RNN.

[4] The blank patches are filtered in the construction of the graph.

3.3 Training and recommendation

The recommendation based on the DPathNet faces the following four issues. 1) The explicit label for each ROI in the path is unavailable in the practical application of SHIR. Therefore, the training of the DPathNet can only utilize the labels of paths. 2) The WSI occasionally contains multiple lesions and thereby the corresponding path is multi-labeled. It determines the network is inappropriate to be trained using class-exclusive loss functions, e.g. cross-entropy. 3) The scale of the recommendation database is growing during the work of the telepathology platform. Therefore, the model should be scalable to the size of the database. 4) The recommendation system is expected to be real-time. The efficiency of the model should be considered.

To simultaneously solve the above issues, we built an encoding layer $\mathbf{c} = \tanh(\mathbf{W}_h\mathbf{h}_n + \mathbf{b}_h)$ at the end of DPathNet to convert the RNN outputs $\mathbf{h}_n$ as binary-like codes, then trained the model using a triplet loss function and finally realized the recommendation based on similarity matching. Specifically, the loss function is defined by the negative log triplet label likelihood [16], which is formulated as

$$\begin{aligned} L = &- \frac{1}{M}\sum_{m=1}^{M}\log\sigma(\frac{1}{2}\mathbf{c}_{a_m}^{\mathrm{T}}\mathbf{c}_{p_m} - \frac{1}{2}\mathbf{c}_{p_m}^{\mathrm{T}}\mathbf{c}_{n_m} - \alpha) \\ &+ \lambda\frac{1}{M}\sum_{m=1}^{M}\sum_{k\in\{a_m,p_m,b_m\}}\|\mathbf{c}_k - \mathbf{u}_k\|_2^2, \end{aligned} \tag{2}$$

where $(\mathbf{c}_{a_m}, \mathbf{c}_{p_m}, \mathbf{c}_{n_m})$ denotes the code of (anchor, relevant, irrelevant) paths for the m-th triplet, M is the number of training paths, α is defined as the margin in the triplet loss, $\sigma(\cdot)$ is the sigmoid function to generate the probability, and $\mathbf{u}_k = sign(\mathbf{c}_k)$ is the binarization code of $\mathbf{c}_k$. The GCN and the RNN in the DPathNet are jointly trained by integrated backward propagation. The gradient optimization algorithm was mini-batch Stochastic Gradient Descent (SGD) with momentum.

The recommendation is achieved by the binary code $\mathbf{u}$ with the similarity measurement based on Hamming distance [11,20].The cases having the most similar binary codes to the path at a certain time are returned as the recommendation results for the time.

4 Experiment

4.1 Experimental settings

To study the feasibility and effectiveness of the SHIR approach, we collected a gastric WSI dataset containing 983 gastric cases. One conclusive WSI was selected from each case to build the WSI dataset. We invited pathologists to make diagnoses for the WSIs on the digital pathology platform[5]. The browsing paths

[5] https://gallery.motic.com

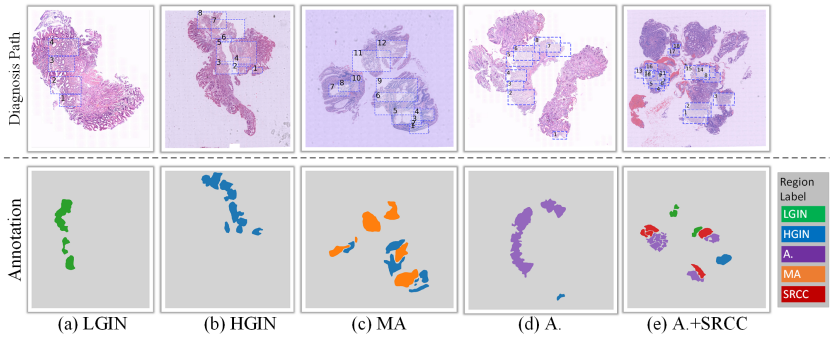

Fig. 3. Display of the gastric database, where the first row displays the diagnosis paths (the regions are numbered in chronological order) traced by telepathology platform, the second row provides the annotations with the notes on the right, and the path labels are provided under the annotations.

of the pathologists were recorded by the platform during the diagnoses and then supplied for this research. Specifically, the screens *focused* on by the pathologists above 10× lenses (0.96μm/pixel) were recorded to the sequential path data. A screen is recognized as *focused* when the display rendering is completed after all the tiles within the screen are downloaded from the cloud. Owning to the second level cache mechanism of the browsing system, small movement and zoom or the revisit to a certain screen will not trigger the rendering and thereby will not repeatedly recorded to the path.

To comprehensively evaluate the proposed model and assess the corresponding full-supervision methods, we invited experts to annotate the exact lesion regions associated to the path and categorize the annotations into 5 types of gastric pathology (including *Low-grade intraepithelial neoplasia* (LGIN), *High-grade intraepithelial neoplasia* (HGIN), *Adenocarcinoma* (A.), *Mucinous adenocarcinoma* (MA), and *Signet-ring cell carcinoma* (SRCC)). The paths were labeled following the priority A.=MA=SRCC>HGIN>LGIN according to the annotation of ROIs in the path. A path was assigned multiple labels if and only it contained more than one malignant tumors (A.,MA, and SRCC), and otherwise, it was assigned a single label. The lengths of the paths range from 1 to 61 with an average number of 10.20. The total number of focused views (i.e., ROIs) is 10030. Several instances from the dataset are presented in Figure 3.

The WSIs in the dataset are divided into subsets as ($\mathcal{D}_{train}$, $\mathcal{D}_{val}$, $\mathcal{D}_{test}$) in number of $(550, 138, 295)$ cases. $\mathcal{D}_{train}$ was used to train the DPathNet and regarded as the recommendation database in the experiment, $\mathcal{D}_{val}$ was used to tune the hyper-parameters involved in the model, and $\mathcal{D}_{test}$ was used as the query set and to assess of the final performance of the SHIR framework. A pair of paths were considered as relevant in both the training and in the evaluation phases if the intersection set of their labels is nonempty and as irrelevant otherwise. The precision for recommending N items (P@N), mean reciprocal rank (MRR) and mean average precision (MAP) for the recommendation were the metrics.

The EfficientNet-b0 structure pre-trained on the ImageNet was employed to extract the patch features. The size of patches is 224×224 to fit the input size of EfficientNet. The hyper-parameters for the GCN model were set referring to [20]. The naive RNN module and LSTM were also evaluated besides GRU.

All the algorithms were implemented in python with torch and run on a computer with 2 CPUs of Intel Xeon E5-2630 and 4 GPUs of Nvidia Geforce 2080Ti. The parameters in the DPathNet are jointly trained by integrated backward propagation. The mini-batch data for each step of training was generated by weighted sampling to ensure a balanced distribution of category labels. The paths in a mini-batch were padded to the maximum path length in the batch. More details please refer to the source code at `https://github.com/Zhengyushan/dpathnet`.

4.2 Results and discussion

The performance of the proposed recommendation framework is presented in Table 1, where the results for the binary-category (malignancy *vs*. benign) recommendation task are also compared. To quantitatively assess the gap of the path-level supervision from the pixel-wise annotation, we made full use of the pixel-wise annotation to pre-train the EfficientNet and the GCN by image patch and ROI classification tasks, respectively, and then fine-tuned the GCN during the training of the DPathNet. The corresponding results (noted by *Pixel* in Table 1) were considered as the upper boundary of the recommendation problem. Table 1 shows that the DPathNet within GRU module achieves an MAP of 0.777 for the 5-category recommendation task (0.921 for the binary task), which is 0.015 (0.014) to the networks trained by pixel-level annotations. The results have indicated 1) The proposed DPathNet is effective in the SHIR task and is promising to build automatic learning systems for telepathology platforms. 2) The path-level (i.e., the WSI-level) supervision is basically sufficient to train the DPathNet. The workload of manual annotation of the pathologist can be entirely relieved at the cost of less than 2% decrease of the recommendation accuracy.

Then, we compared the proposed method with 3 related works [15,20,18]. The method [15] studies WSI retrieval. We adopted the algorithm in [15] to achieve diagnosis path recommendation. Yan et al. [18] utilized an RNN to classify histopathological images and Zheng et al. [20] applied GCNs to encoding sub-regions on the WSI. In this experiment, we trained the networks in the two methods based on the ROI labels to extracted ROI features. Meanwhile, we adapted the patch-based similarity measurement proposed in [15] to these ROI features to realize the recommendation. The results are given in Table 2. Overall, the proposed DPathNet performed significantly better than the compared methods. The supervision (ROI label) in [18] and [20] is stronger than that in DPathNet but the two methods do not consider the sequential information of ROIs in the diagnosis path. Therefore, the results of the two methods cannot surpass DPathNet. In comparison, DPathNet has modeled the sequential information using an RNN structure. The high level of pathology knowledge for lesion recognition has been learned from the context relationship within the diagnosis

Table 1. Comparison of the recommendation metrics for different levels of supervision. Please refer to the text for detail.

Methods	Label type	Binary task				5-category task			
		P@5	P@20	MRR	MAP	P@5	P@20	MRR	MAP
DPathNet w/ RNN	*Pixel*	0.919	0.910	0.937	0.938	0.736	0.736	0.760	0.784
DPathNet w/ LSTM	*Pixel*	0.906	0.903	0.912	0.931	0.749	0.752	0.775	0.792
DPathNet w/ GRU	*Pixel*	0.909	0.912	0.922	0.937	0.755	0.749	0.773	0.784
DPathNet w/ RNN	*WSI*	0.860	0.864	0.874	0.898	0.626	0.629	0.696	0.659
DPathNet w/ LSTM	*WSI*	0.887	0.889	0.888	0.921	0.691	0.684	0.725	0.760
DPathNet w/ GRU	*WSI*	0.892	0.897	0.911	0.924	0.716	0.707	0.741	0.777

Table 2. Comparison of the recommendation metrics for relevant approaches and the proposed method. Please refer to the text for detail.

Methods	Binary task				5-category task			
	P@5	P@20	MRR	MAP	P@5	P@20	MRR	MAP
Jimenez-del-Toro et al. [15]	0.795	0.811	0.883	0.818	0.632	0.622	0.692	0.655
Yan et al. [18]	<u>0.859</u>	0.849	0.904	0.862	<u>0.678</u>	<u>0.664</u>	<u>0.726</u>	0.702
Zheng et al. [20]	0.834	<u>0.858</u>	**0.915**	<u>0.881</u>	0.654	0.659	0.721	<u>0.712</u>
DPathNet (Ours)	**0.892**	**0.897**	<u>0.911</u>	**0.924**	**0.716**	**0.707**	**0.741**	**0.777**

path, and thereby delivered better recommendation performance. The average time for a step of recommendation when a new screen was appended to the path was 474.84 ms, which is promising to develop near real-time applications.

Figure 4 illustrates 3 recommendation instances of the proposed SHIR framework. Generally, the recommendation for lesion types A. and SRCC are acceptable. The accuracy for the type HGIN occasionally confused with the LGIN and A. in its present version, which needs to be improved in future work.

5 Conclusion

The browse paths of pathologists on the whole slide images are valuable information, which is highly correlated with the diagnosis of cancer cases yet can be easily recorded by the digital pathology platform. In this paper, we developed a novel DPathNet to model the path information on the WSI. Meanwhile, we proposed a novel computer-aided cancer diagnosis framework named session-based histopathological image recommendation (SHIR) based on the DPathNet. The experiments have shown that the DPathNet has successfully learned the pathology knowledge by only using the diagnosis paths, for which the workload of manually annotation can be significantly relieved. The results on the gastric dataset indicates that the DPathNet is a promising to develop SHIR system for telepathology platform.

Acknowledgment

This work was partly supported by the National Natural Science Foundation of China (Grant No. 61901018, 61771031, and 61906058), partly by China Postdoc-

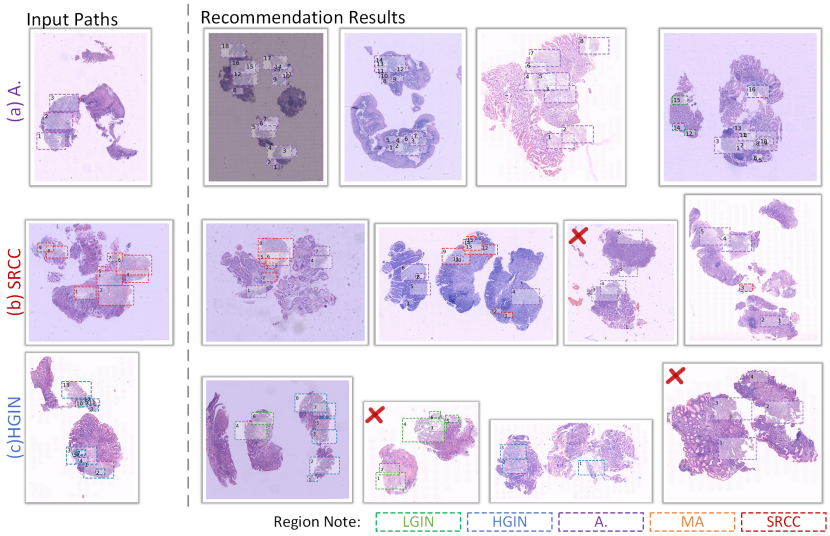

Fig. 4. The illustration of recommendation results, where first column displays 3 instances in the testing set with the path label provided on the left, the top recommendation results for each instance is are displayed on the right, and the incorrect results (irrelevant to the input one) are marked by red cross.

toral Science Foundation (No. 2019M650446) and partly by Motic-BUAA Image Technology Research Center.

References

1. Bejnordi, B.E., Veta, M., Van Diest, P.J., Van Ginneken, B., Karssemeijer, N., Litjens, G., Van Der Laak, et al.: Diagnostic assessment of deep learning algorithms for detection of lymph node metastases in women with breast cancer. JAMA **318**(22), 2199–2210 (2017)
2. Campanella, G., Hanna, M.G., Geneslaw, L., Miraflor, A., Silva, V.W.K., Busam, K.J., Brogi, E., Reuter, V.E., Klimstra, D.S., Fuchs, T.J.: Clinical-grade computational pathology using weakly supervised deep learning on whole slide images. Nature medicine **25**(8), 1301–1309 (2019)
3. Cho, K., van Merriënboer, B., Gulcehre, C., Bahdanau, D., Bougares, F., Schwenk, H., Bengio, Y.: Learning phrase representations using rnn encoder–decoder for statistical machine translation. In: Proceedings of the 2014 Conference on Empirical Methods in Natural Language Processing (EMNLP). pp. 1724–1734 (2014)
4. Hollon, T.C., Pandian, B., Adapa, A.R., Urias, E., Save, A.V., Khalsa, S.S.S., Eichberg, D.G., D'Amico, R.S., Farooq, Z.U., Lewis, S., et al.: Near real-time intraoperative brain tumor diagnosis using stimulated raman histology and deep neural networks. Nature Medicine **26**(1), 52–58 (2020)
5. Hu, D., Zheng, Y., Zhang, H., Sun, S., Xie, F., Shi, J., Jiang, Z.: Informative retrieval framework for histopathology whole slides images based on deep hashing network. In: 2020 IEEE 17th International Symposium on Biomedical Imaging (ISBI). pp. 244–248 (2020)

6. Kalra, S., Tizhoosh, H., Choi, C., Shah, S., Diamandis, P., Campbell, C.J., Pantanowitz, L.: Yottixel – an image search engine for large archives of histopathology whole slide images. Medical Image Analysis p. 101757 (2020)
7. Van der Laak, J., Ciompi, F., Litjens, G.: No pixel-level annotations needed. Nature Biomedical Engineering **3**(11), 855–856 (2019)
8. Li, R., Yao, J., Zhu, X., Li, Y., Huang, J.: Graph cnn for survival analysis on whole slide pathological images. In: International Conference on Medical Image Computing and Computer-Assisted Intervention. pp. 174–182. Springer (2018)
9. Li, Z., Zhang, X., Müller, H., Zhang, S.: Large-scale retrieval for medical image analytics: A comprehensive review. Medical image analysis **43**, 66–84 (2018)
10. Liu, Q., Zeng, Y., Mokhosi, R., Zhang, H.: Stamp: short-term attention/memory priority model for session-based recommendation. In: Proceedings of the 24th ACM SIGKDD International Conference on Knowledge Discovery & Data Mining. pp. 1831–1839 (2018)
11. Peng, T., Boxberg, M., Weichert, W., Navab, N., Marr, C.: Multi-task learning of a deep k-nearest neighbour network for histopathological image classification and retrieval. In: International Conference on Medical Image Computing and Computer-Assisted Intervention. pp. 676–684. Springer (2019)
12. Sapkota, M., Shi, X., Xing, F., Yang, L.: Deep convolutional hashing for low-dimensional binary embedding of histopathological images. IEEE journal of biomedical and health informatics **23**(2), 805–816 (2018)
13. Shi, X., Sapkota, M., Xing, F., Liu, F., Cui, L., Yang, L.: Pairwise based deep ranking hashing for histopathology image classification and retrieval. Pattern Recognition **81**, 14–22 (2018)
14. Tan, M., Le, Q.: Efficientnet: Rethinking model scaling for convolutional neural networks. In: International Conference on Machine Learning. pp. 6105–6114 (2019)
15. Jimenez-del Toro, O., Otálora, S., Atzori, M., Müller, H.: Deep multimodal case–based retrieval for large histopathology datasets. In: MICCAI 2018 Workshop on Patch-based Techniques in Medical Imaging. pp. 149–157. Springer (2017)
16. Wang, X., Shi, Y., Kitani, K.M.: Deep supervised hashing with triplet labels. In: Asian conference on computer vision. pp. 70–84. Springer (2016)
17. Wu, S., Tang, Y., Zhu, Y., Wang, L., Xie, X., Tan, T.: Session-based recommendation with graph neural networks. In: Proceedings of the AAAI Conference on Artificial Intelligence. vol. 33, pp. 346–353 (2019)
18. Yan, R., Ren, F., Wang, Z., Wang, L., Zhang, T., Liu, Y., Rao, X., Zheng, C., Zhang, F.: Breast cancer histopathological image classification using a hybrid deep neural network. Methods (2019)
19. Ying, Z., You, J., Morris, C., Ren, X., Hamilton, W., Leskovec, J.: Hierarchical graph representation learning with differentiable pooling. In: Advances in neural information processing systems. pp. 4800–4810 (2018)
20. Zheng, Y., Jiang, B., Shi, J., Zhang, H., Xie, F.: Encoding histopathological wsis using gnn for scalable diagnostically relevant regions retrieval. In: International Conference on Medical Image Computing and Computer-Assisted Intervention. pp. 550–558. Springer (2019)
21. Zheng, Y., Jiang, Z., Zhang, H., Xie, F., Ma, Y., Shi, H., Zhao, Y.: Histopathological whole slide image analysis using context-based cbir. IEEE transactions on medical imaging **37**(7), 1641–1652 (2018)
22. Zheng, Y., Jiang, Z., Zhang, H., Xie, F., Ma, Y., Shi, H., Zhao, Y.: Size-scalable content-based histopathological image retrieval from database that consists of wsis. IEEE journal of biomedical and health informatics **22**(4), 1278–1287 (2018)